Corrections to the Dielectric Constant of a Degenerate Electron Gas

ARNOLD J. GLICK
University of Maryland, College Park, Maryland
(Received 7 September 1962)

The Lindhard approximation to the frequency- and wave-number dependent dielectric constant, $\epsilon(\mathbf{k},\omega)$, provides a good description of many properties of the degenerate electron gas. However, it is known that the short-range behavior of the gas is not adequately represented by this function and it is necessary to include certain additional terms. DuBois incorporated some exchange terms into $\epsilon(\mathbf{k},\omega)$ and was able to obtain the correction to the plasmon excitation frequency. Though his final results are reasonable and have been corroborated using alternative approaches the "corrected" dielectric constant is found to violate certain *a priori* restrictions. In this paper a more accurate dielectric constant is derived. In order to obtain an acceptable function which does not violate the sum rule and positive definiteness restrictions on the imaginary part it is necessary to account for three types of corrections. These corrections originate in (1) the effective screening of the long-range interaction between particles; (2) the shift in single-particle energies of electrons and holes; and (3) the tendency of particles and holes to form bound states when any repulsive interparticle interaction is present. With these corrections all spurious singularities in the dielectric constant disappear. Numerical calculations of $\epsilon(\mathbf{k},\omega)$ and of moments of the imaginary part of this function have been carried out for an intermediate electron density equal to the density of conduction electrons in aluminum. The resulting dielectric constant departs by as much as 50% from the Lindhard form for low frequencies, but has similar qualitative features. The moments can be used to determine the high-frequency behavior and other properties of the electron gas.

I. INTRODUCTION

THE dielectric formulation of the many-body problem has been found to be very useful in treating the degenerate electron gas and for studying properties of solids which depend strongly on electron-electron interactions.[1–4] The frequency- and wave-number-dependent dielectric constant can be used to rigorously describe and relate many properties of the system. These properties include any that can be expressed in terms of an expectation value of a two-body operator, or in terms of the rate of transitions out of the ground state induced by a one-body operator or external field acting on the system.[5] Thus, this approach has been applied in analyses of electron scattering by thin metal films[2,3,6]; and for studying the pair distribution function and the ground-state energy of the degenerate electron gas, and the nature of the plasmon excitation mode. It has also been shown[7,8] that the effective interaction between electrons, ions, or impurities in the system can be expressed in terms of the dielectric constant. This function, in effect, transforms the elementary two-body Coulomb force into a non-local, time-dependent interaction which incorporates the complicated screening effects of the intervening electron gas. Experimental studies of many phenomena in solids have recently been refined to the point where it has become interesting and necessary for theory to incorporate the effects of these electron-electron interactions.

However, the dielectric constants used in previous studies are not completely satisfactory and violate certain *a priori* restrictions. Using the dielectric constant first found by Lindhard,[1] one can obtain a description of screening effects and of the plasmon excitation mode which is very accurate for high electron densities and appears to be quite good even for metallic electron densities. However, it has been shown that short-range effects are badly represented; indeed for metallic densities the pair distribution function found with this approximation becomes negative for small separation between particles.[4,9,10] DuBois[11] calculated an improved dielectric constant valid to the next order in perturbation theory. While perturbation theory cannot be applied to calculations of most properties of the electron gas due to the long-range character of the Coulomb force, it had been suggested[4,7,11] that it might be valid for determining the dielectric constant of the medium. DuBois' dielectric constant does tend to remove the difficulties with the pair distribution function to lower densities, but it is now found that another important condition is violated: The imaginary

* Supported in part by the U. S. Air Force Office of Scientific Research under grant AFOSR–62–46, and by the National Science Foundation while the author was a Postdoctoral Fellow at the Weizmann Institute of Science. A preliminary report on this work was presented at the 1962 Annual Meeting of the American Physical Society [A. J. Glick, Bull. Am Phys. Soc. 7, 67 (1962)].

[1] J. Lindhard, Kgl. Danske Videnskab, Selskab, Mat.-Fys. Medd. 28, 8 (1954).
[2] J. Hubbard, Proc. Phys. Soc. (London) A68, 976 (1955).
[3] P. Nozières and D. Pines, Phys. Rev. 113, 1254 (1959).
[4] A. J. Glick, in "*Lectures on the Many-Body Problems, Naples, 1960*," edited by E. Caianiello (Academic Press Inc., New York, 1962).
[5] A. J. Glick, Ann. Phys. (N. Y.) 17, 61 (1962).
[6] R. H. Ritchie, Phys. Rev. 114, 644 (1959).
[7] J. Hubbard, Proc. Roy. Soc. (London) A240, 539 (1957); A242, 336 (1958).
[8] J. J. Quinn and R. A. Ferrell, Phys. Rev. 112, 812 (1958).
[9] A. J. Glick and R. A. Ferrell, Ann. Phys. (N. Y.) 11, 359 (1960).
[10] D. Pines, *The Many-Body Problem* (W. A. Benjamin, Inc., New York, 1961). In these notes Dr. Pines disagreed with this result, but he has more recently come to agree that it is, indeed, correct (private communication).
[11] D. F. DuBois, Ann Phys. (N. Y.) 7, 174 (1959); 8, 24 (1959).

part of the new dielectric constant becomes negative for certain frequencies.

In this paper, we calculate a more accurate dielectric constant which appears to be free of these difficulties. It is shown that it is not merely the long-range nature of the Coulomb force which causes trouble. For any repulsive interparticle interaction ordinary perturbation theory is inadequate for determining corrections to the dielectric constant valid for all frequencies and small wave numbers. In the present case the breakdown of perturbation theory is due to three different effects of interaction. These are (1) the long range of the Coulomb force; (2) small shifts in single-particle energies and the Fermi surface; (3) the tendency of particles and holes to form a bound state when any repulsive interparticle interaction is present. As a result it is necessary to combine three groups of terms for calculating the dielectric constant.

The method of calculation is the same as that discussed in references 4 and 5. We use a diagrammatic many-body perturbation theory or equivalent Green's function formalism to find the linear response to a density fluctuation. The imaginary part of the dielectric constant is then given by the contributions of the reduced class of diagrams which comprise a "black bubble." We here consider the completely degenerate electron gas, and restrict ourselves to the long-wavelength ($k \rightarrow 0$) limit where the difficulties with the perturbation treatment are most pronounced.

In the next section we consider the corrections given by perturbation theory to Lindhard's dielectric constant[1] and we obtain a function equivalent to that used by DuBois.[11] However, the present derivation gives the imaginary part of the dielectric constant directly and the result evidently violates the *a priori* positive-definiteness condition.

In Sec. III an effective screened interaction is derived from a consideration of higher order processes. With this interaction the divergences associated with the long-range Coulomb force disappear but by itself this improvement does not provide a satisfactory dielectric constant. In Sec. IV the single-particle propagators are modified to incorporate self-energy effects. In this way we eliminate the familiar severe singularities in higher order terms of the perturbation series which are due to small shifts in single-particle energies. In the present approximation this correction can be taken into account by introducing an effective mass into particle and hole energy differences. The effective mass is calculated and found to differ from the electron mass by less than 5% for any electron density.

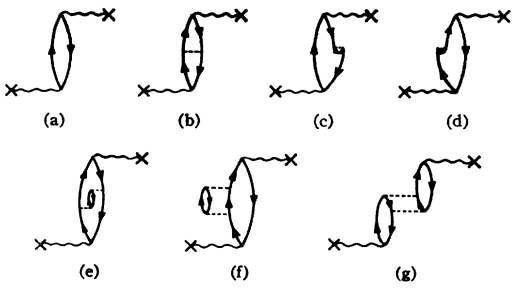

FIG. 1. Typical graphs which contribute to the imaginary part of the dielectric constant. (a) is the graph which reproduces Lindhard's approximation while (b), (c), and (d) represent the first-order corrections which were included by DuBois.

With the effective interaction and effective propagators derived in Secs. III and IV incorporated into the correction terms to the dielectric constant, it still remains necessary to provide for the presence of a pole in the free-particle-hole propagator. Thus, in Sec. V an acceptable dielectric constant is obtained by carrying out a summation over a class of graphs containing repeated particle-hole scatterings. This sum is over graphs which are the exchange counterparts of the familiar simple "bubble graphs." These calculations indicate that even for very small wave numbers where the "direct" terms in perturbation theory would be thought to be very much larger than their individual exchange counterparts, the exchange terms are still sufficiently singular for certain frequencies that they must be combined over all orders to make valid improvements in the calculation. The resulting dielectric constant is well behaved and provides reasonable corrections to results obtained with Lindhard's function. Section VI consists of a short summary.

II. PERTURBATION THEORETIC CORRECTIONS

In reference 4, it was shown that the imaginary part, ϵ_2, of the frequency- and wave-number-dependent dielectric constant, $\epsilon(\mathbf{k},\omega)$ can be expressed in terms of the real part of an integral over positive t which takes the form ($\hbar$ equal to unity)

$$\epsilon_2(\mathbf{k},\omega)=\frac{v(\mathbf{k})}{\Omega}\,\mathrm{Re}\int_0^\infty dt\,(e^{i\omega t}-e^{-i\omega t}) \times\langle\Psi_0|\rho_{\mathbf{k}}^\dagger(t)\rho_{\mathbf{k}}(0)|\Psi_0\rangle_B, \quad (2.1)$$

where $v(\mathbf{k})$ is the Fourier transform of the interparticle interaction, Ω is the quantization volume, $\rho_{\mathbf{k}}(t)$ is the Heisenberg density fluctuation operator:

$$\rho_{\mathbf{k}}(t)=e^{iHt}\rho_{\mathbf{k}}e^{-iHt},$$
$$\rho_{\mathbf{k}}=\sum_{\mathbf{k}} e^{i\mathbf{k}\cdot\mathbf{r}},$$

and Ψ_0 and H are the many-particle interacting ground state and Hamiltonian of the system. The rules for drawing diagrams and finding their contributions to the matrix element in (2.1) were given in reference 4, but for convenience we include a momentum space form of the rules in Appendix A. The subscript B on the matrix element refers to the graphical description and restricts the contributions to terms coming from the "black bubble" graphs, i.e., those which cannot be divided into two unlinked parts by cutting a single interaction line. Typical contributing graphs are shown in Fig. 1. The

real part, ϵ_1, of the dielectric constant can then be found from the Kramers-Kronig dispersion relation,

$$\epsilon_1(\mathbf{k},\omega)=1+\frac{2}{\pi}\mathcal{P}\int_0^\infty \frac{\omega'\epsilon_2(\mathbf{k},\omega')}{\omega'^2-\omega^2}d\omega'. \tag{2.2}$$

The contribution from Fig. 1(a) gives Lindhard's[1] dielectric constant $\epsilon^L(\mathbf{k},\omega)$. As $\mathbf{k}$ approaches zero this result reduces to

$$\epsilon_2{}^L(\mathbf{k},\omega)\underset{\mathbf{k}\to 0}{\longrightarrow}\frac{2k_0}{a_0k^2}u\,\eta(1-|u|), \tag{2.3}$$

where $u=\omega/(kv_0)$ with v_0 denoting the Fermi velocity,

$$\begin{aligned}\eta(x)&=1, \quad \text{for} \quad x>0\\ &=0, \quad \text{for} \quad x<0,\end{aligned} \tag{2.4}$$

and $a_0=1/(me^2)$.

The first-order corrections to (2.3) come from the graphs shown in Figs. 1(b), (c), and (d). Applying the rules of Appendix A and integrating out the variables restricted by the δ functions, we find the following contributions to the matrix element:

$$\text{M.E.}^{1b}=-\frac{1}{4\pi^3i\Omega}\sum_{\mathbf{k}_1,\mathbf{k}_2}\int_{-\infty}^{\infty}d\omega_1d\omega_2d\omega'\times e^{-i\omega' t}v(\mathbf{k}_1-\mathbf{k}_2)S(\mathbf{k}_1,\omega_1)S(\mathbf{k}_1-\mathbf{k},\,\omega_1-\omega')\times S(\mathbf{k}_2,\omega_2)S(\mathbf{k}_2-\mathbf{k},\,\omega_2-\omega'), \tag{2.5a}$$

$$\begin{aligned}&\text{M.E.}^{1c}+\text{M.E.}^{1d}\\ &=-\frac{1}{4\pi^3i\Omega}\sum_{\mathbf{k}_1,\mathbf{k}_2}\int_{-\infty}^{\infty}d\omega_1d\omega_2d\omega'\,e^{-i\omega' t}v(\mathbf{k}_1-\mathbf{k}_2)\\ &\quad\times S(\mathbf{k}_1,\omega_1)S(\mathbf{k}_1,\omega_1)S(\mathbf{k}_2,\omega_2)\\ &\quad\times[S(\mathbf{k}_1-\mathbf{k},\,\omega_1-\omega')+S(\mathbf{k}_1+\mathbf{k},\,\omega_1+\omega')].\end{aligned} \tag{2.5b}$$

The integrations over the ω_i can be carried out using the simple structure of the particle propagators $S(\mathbf{k}_i,\omega_i)$ given by Eq. (A1). After substitution into (2.1), the integrations over t and ω are easily performed as indicated in Appendix B and the first-order corrections to ϵ_2 become

$$\epsilon_2{}^{1b}=-\frac{4\pi v(\mathbf{k})}{\Omega^2}\sum_{\mathbf{k}_1,\mathbf{k}_2}\eta_{\mathbf{k}_1>}\eta_{\mathbf{k}_1-\mathbf{k}<}\eta_{\mathbf{k}_2>}[\delta(\omega-E_{\mathbf{k}_1}+E_{\mathbf{k}_1-\mathbf{k}})-\delta(\omega+E_{\mathbf{k}_1}-E_{\mathbf{k}_1-\mathbf{k}})]\times\left\{\frac{v(\mathbf{k}_1-\mathbf{k}_2-\mathbf{k})\eta_{\mathbf{k}_2+\mathbf{k}<}}{E_{\mathbf{k}_2+\mathbf{k}}-E_{\mathbf{k}_2}-E_{\mathbf{k}_1}+E_{\mathbf{k}_1-\mathbf{k}}}-\mathcal{P}\frac{v(\mathbf{k}_1-\mathbf{k}_2)\eta_{\mathbf{k}_2-\mathbf{k}<}}{E_{\mathbf{k}_2}-E_{\mathbf{k}_2-\mathbf{k}}-E_{\mathbf{k}_1}+E_{\mathbf{k}_1-\mathbf{k}}}\right\}, \tag{2.6a}$$

$$\epsilon_2{}^{1c}+\epsilon_2{}^{1d}=\frac{2\pi v(\mathbf{k})}{\Omega^2}\sum_{\mathbf{k}_1,\mathbf{k}_2}\eta_{\mathbf{k}_1>}\eta_{\mathbf{k}_1-\mathbf{k}<}\eta_{\mathbf{k}_2<}[\delta'(\omega-E_{\mathbf{k}_1}+E_{\mathbf{k}_1-\mathbf{k}})+\delta'(\omega+E_{\mathbf{k}_1}-E_{\mathbf{k}_1-\mathbf{k}})][v(\mathbf{k}_1-\mathbf{k}_2)-v(\mathbf{k}_1-\mathbf{k}_2-\mathbf{k})], \tag{2.6b}$$

where $\mathcal{P}$ denotes principal part in the integration over the pole in the denominator of (2.6a) and the $\eta_{\mathbf{k}>}$ and $\eta_{\mathbf{k}<}$ are defined in Appendix A; note that Eq. (2.6b) contains a derivative of the δ function with respect to ω. For the electron gas the interparticle interaction takes the form

$$v(\mathbf{k})=4\pi e^2/k^2. \tag{2.7}$$

The sums over $\mathbf{k}_1$ and $\mathbf{k}_2$ can be replaced by integrals which are easily evaluated in the limit $k\to 0$ for which the regions of integration collapse into very thin caps on the Fermi sphere.[12]

Combining Eqs. (2.6), the correction to ϵ_2 can be written in the form

$$\Delta\epsilon_2=\frac{1}{\pi a_0{}^2k^2}\left\{\left[6u+\frac{1}{1+u}-\frac{1}{1-u}\right]\eta(1-|u|)+\frac{|u|}{u}\left[\ln\left(\frac{2}{1-|u|}\right)-4\right]\delta(1-|u|)\right\}. \tag{2.8}$$

Though this result is very singular, it is integrable. Substituting into (2.2) we obtain

$$\Delta\epsilon_1=\frac{1}{\pi^2a_0{}^2k^2}\left\{\left(6u+\frac{1}{1+u}-\frac{1}{1-u}\right)\ln\left|\frac{1-u}{1+u}\right|+12-\frac{4}{1-u}-\frac{4}{1+u}\right\}, \tag{2.9}$$

which corresponds to the correction to the polarization propagator found by DuBois[13] from graphs analogous to Figs. 1(b), (c), and (d).

As shown in reference 9, it is also of interest to know the u moments of the differential oscillator strength df_k/du,

$$df_k/du=2u\epsilon_2/(\pi u_p{}^2), \tag{2.10}$$

with

$$u_p{}^2=\omega_p{}^2/(kv_0)^2=4\pi ne^2/(mk^2v_0{}^2)=4k_0/(3\pi a_0k^2). \tag{2.11}$$

The zeroth moment is fixed by the well-known sum rule,

$$\int_0^\infty du\,u\epsilon_2=\pi u_p{}^2/2. \tag{2.12}$$

[12] In (2.6b) the $\eta_{\mathbf{k}_2-\mathbf{k}>}$ does not appear directly from application of the rules but the effect of cancellation between the first and second $v(\mathbf{k})$'s gives the same effect.

[13] D. F. DuBois, Ann. Phys. (N. Y.) 7, 174 (1959), Appendix A.

Since Lindhard's function (2.3) already exhausts this sum rule, the contribution of corrections to ϵ_2 to the zeroth moment should vanish. This condition is, indeed, satisfied by (2.8). Calculating the correction to the higher moments, one easily finds

$$\Delta\langle u^n\rangle \equiv \frac{2}{\pi u_p^2}\int_0^\infty u^n u \Delta\epsilon_2 du, \tag{2.13}$$

$$\Delta\langle u^2\rangle = -1/5\pi k_0 v_0, \tag{2.14}$$

$$\Delta\langle u^4\rangle = -4/35\pi k_0 a_0, \tag{2.15}$$

which can be compared with the small-k result of reference 9,

$$\langle u^2\rangle_{k\to 0} = 3/5, \tag{2.16}$$

$$\langle u^4\rangle_{k\to 0} = 3/7. \tag{2.17}$$

Using (2.14) we can substitute into Eq. (20) of reference 9 to obtain the "exchange correction" to the plasmon frequency. The result is in agreement with that found by DuBois[11] and others, giving to order k^2

$$\omega_k/\omega_p = 1+(9\pi k_0 a_0/40)(k^2/k_0^2)(1-1/3\pi k_0 a_0). \tag{2.18}$$

Similarly one can use Eq. (25) of reference 9 to find the plasmon oscillator strength which becomes, to order k^4,

$$\int_{\text{pl}} dF_k = 1-\frac{27\pi^2 k_0^2 a_0^2}{700}\frac{k^4}{k_0^4} \times\left[1+\frac{11}{6\pi k_0 a_0}-\frac{7}{12\pi^2 k_0^2 a_0^2}\right]. \tag{2.19}$$

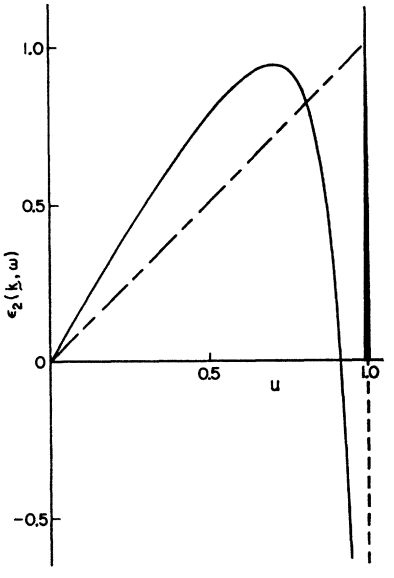

FIG. 2. Imaginary part of the dielectric constant in units of $2k_0/(a_0k^2)$ as given by first-order perturbation theory and plotted as a function of u for an electron density equal to the density of conduction electrons in aluminum. Note that this function violates the *a priori* positive-definiteness condition for $u\approx 1$ and also has a δ-function peak with infinite coefficient at $u=1$. The broken line shows ϵ_2 in the zero-order (Lindhard) approximation. Both forms of ϵ_2 vanish for $u>1$.

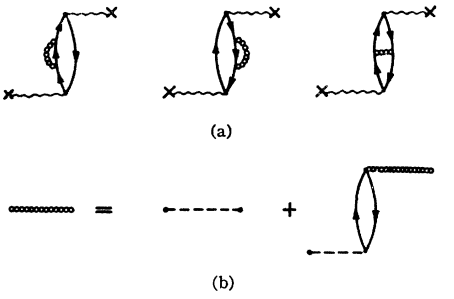

FIG. 3. (a) First-order irreducible graphs which contribute to the dielectric constant when an effectively screened interaction is used. The chains represent the approximate interaction which is found from an integral equation represented schematically in (b).

These corrections to the plasmon frequency and strength are small for high densities and are even reasonable for metallic densities. For a density equal to the density of conduction electrons in aluminum one has $1/(\pi k_0 a_0)\approx 0.34$.

Note, however, that $\Delta\epsilon_2$ is highly singular, and in the region of $u=1$ this function becomes much larger than the zero-order term given by (2.3). Thus, for small k and u near unity it appears that perturbation theory fails. Indeed, as shown in Fig. 2, the imaginary part of the dielectric constant is driven negative in this approximation in violation of an *a priori* restriction. A negative value of ϵ_2 for positive frequencies implies that the system generates rather than absorbs energy on excitation from the ground state. Such a result indicates either that we have incorrectly chosen the ground state and there actually are other states of lower energy, or that perturbation theory has broken down and gives meaningless results in this frequency range. Since the Coulomb interaction between particles is repulsive, it is unlikely that there exist states of lower energy than the normal ground state. Hence, we are concerned in the remainder of this paper with the derivation of a more accurate correction to ϵ_2, which seems to be in better accord with the *a priori* criteria at our disposal.

III. THE EFFECTIVE INTERACTION

A frequent cause of the failure of perturbation theory, when applied to the electron gas, is the long-range nature of the Coulomb force. However, for the determination of ϵ_2 it is shown in this section that perturbation theory is unsuccessful even with a screened interaction between particles. We first investigate how certain higher order processes introduce an effectively screened interaction and then we reconsider the graphs of the previous section as modified by the effective interaction for calculating a screened $\Delta\epsilon_2$.

Hubbard[7] has shown how the perturbation series which we have been using can be formally rearranged in terms of the effective interaction. One then restricts attention to a class of irreducible graphs (to avoid

counting contributions more than once), and the effective interaction is determined as a sum over all possible graph parts which begin and end with a simple interaction line, but have no other external lines. It has been shown[7,11] that the only modification in the rules of Appendix A in this treatment is that in rule 1 the interaction $v(\mathbf{k}_i)$ is replaced by

$$\mathcal{U}(\mathbf{k}_i,\omega_i)=v(\mathbf{k}_i)/\tilde{\epsilon}(\mathbf{k}_i,\omega_i), \tag{3.1}$$

where $\tilde{\epsilon}(\mathbf{k}_i,\omega_i)$ is the exact dielectric constant of the system except that its imaginary part has opposite sign for negative ω_i, i.e.,

$$\tilde{\epsilon}(\mathbf{k},\omega)=\tilde{\epsilon}(\mathbf{k},-\omega), \tag{3.2}$$

whereas

$$\epsilon(\mathbf{k},\omega)=\epsilon(\mathbf{k},-\omega)^*. \tag{3.3}$$

The first-order irreducible graphs which contribute to ϵ_2 are shown in Fig. 3(a). Since the effective interaction is not instantaneous these graphs represent more time orderings than do Figs. 1(b), (c), and (d). However, the additional contributions are characterized by terms of the form

$$\frac{1}{\omega'+E_{\mathbf{k}_1-\mathbf{k}}-E_{\mathbf{k}_1}}\frac{1}{\omega'+E_{\mathbf{k}_2-\mathbf{k}}-E_{\mathbf{k}_2}-i\alpha}[\mathcal{U}_-(\mathbf{k}_1-\mathbf{k}_2;E_{\mathbf{k}_1}-E_{\mathbf{k}_2})-\mathcal{U}_-(\mathbf{k}_1-\mathbf{k}_2;\omega'+E_{\mathbf{k}_1-\mathbf{k}}-E_{\mathbf{k}_2})],$$

containing a difference between $\mathcal{U}_-$'s or $\mathcal{U}_+$'s, where $\mathcal{U}_-(\mathbf{k},\omega)$ and $\mathcal{U}_+(\mathbf{k},\omega)$ are those parts of $\mathcal{U}(\mathbf{k},\omega)$ which are analytic in the lower and upper half of the complex ω plane, respectively.[4] Note also that the ω' dependence is such that the terms tend to cancel when the denominators are small. We, therefore, neglect these additional contributions compared to those which contain terms of the form

$$\frac{1}{\omega'+E_{\mathbf{k}_1-\mathbf{k}}-E_{\mathbf{k}_1}+i\alpha}\frac{1}{\omega'+E_{\mathbf{k}_2-\mathbf{k}}-E_{\mathbf{k}_2}+i\alpha}[\mathcal{U}_-(\mathbf{k}_1-\mathbf{k}_2;E_{\mathbf{k}_1}-\omega'-E_{\mathbf{k}_2-\mathbf{k}})+\mathcal{U}_+(\mathbf{k}_1-\mathbf{k}_2;\omega'+E_{\mathbf{k}_1-\mathbf{k}}-E_{\mathbf{k}_2})].$$

In this latter case the denominators enhance the contributions for ω' such that the bracketed expression can be approximately taken as

$$[\mathcal{U}_-(\mathbf{k}_1-\mathbf{k}_2;E_{\mathbf{k}_1}-E_{\mathbf{k}_2})+\mathcal{U}_+(\mathbf{k}_1-\mathbf{k}_2;E_{\mathbf{k}_1}-E_{\mathbf{k}_2})]=\mathcal{U}(\mathbf{k}_1-\mathbf{k}_2;E_{\mathbf{k}_1}-E_{\mathbf{k}_2}). \tag{3.4}$$

Replacing the effective interaction by its value where the coefficient peaks, we obtain an expression for the screened $\Delta\epsilon_2$ which is very similar to (2.6),

$$\begin{aligned}\Delta\epsilon_2{}^S=&-\frac{4\pi v(\mathbf{k})}{\Omega^2}\sum_{\mathbf{k}_1,\mathbf{k}_2}\eta_{\mathbf{k}_1>}\eta_{\mathbf{k}_1-\mathbf{k}<}\eta_{\mathbf{k}_2>}[\delta(\omega-E_{\mathbf{k}_1}+E_{\mathbf{k}_1-\mathbf{k}})-\delta(\omega+E_{\mathbf{k}_1}-E_{\mathbf{k}_1-\mathbf{k}})]\\&\times\left\{\frac{\mathcal{U}(\mathbf{k}_1-\mathbf{k}_2;E_{\mathbf{k}_1-\mathbf{k}}-E_{\mathbf{k}_2})\eta_{\mathbf{k}_2+\mathbf{k}<}}{E_{\mathbf{k}_2+\mathbf{k}}-E_{\mathbf{k}_2}-E_{\mathbf{k}_1}+E_{\mathbf{k}_1-\mathbf{k}}}\mathcal{P}\frac{\mathcal{U}(\mathbf{k}_1-\mathbf{k}_2;E_{\mathbf{k}_1}-E_{\mathbf{k}_2})\eta_{\mathbf{k}_2-\mathbf{k}<}}{E_{\mathbf{k}_2}-E_{\mathbf{k}_2-\mathbf{k}}-E_{\mathbf{k}_1}+E_{\mathbf{k}_1-\mathbf{k}}}\right\}\\&+\frac{2\pi v(\mathbf{k})}{\Omega^2}\sum_{\mathbf{k}_1,\mathbf{k}_2}\eta_{\mathbf{k}_1>}\eta_{\mathbf{k}_1-\mathbf{k}<}\eta_{\mathbf{k}_2<}[\delta'(\omega-E_{\mathbf{k}_1}+E_{\mathbf{k}_1-\mathbf{k}})+\delta'(\omega+E_{\mathbf{k}_1}-E_{\mathbf{k}_1-\mathbf{k}})]\\&\times[\mathcal{U}(\mathbf{k}_1-\mathbf{k}_2;E_{\mathbf{k}_1}-E_{\mathbf{k}_2})-\mathcal{U}(\mathbf{k}_1-\mathbf{k}_2-\mathbf{k};E_{\mathbf{k}_1-\mathbf{k}}-E_{\mathbf{k}_2-\mathbf{k}})].\end{aligned} \tag{3.5}$$

For our purpose a sufficiently accurate effective interaction can be found from the integral equation represented by Fig. 3(b). Its solution is well known and can be written in the form (3.1) with $\tilde{\epsilon}(\mathbf{k}_i,\omega_i)$ given by Linhard's[1] function $\tilde{\epsilon}^L(\mathbf{k}_i,\omega_i)$. But we need not retain the full and complicated dependence of $\tilde{\epsilon}^L(\mathbf{k}_i,\omega_i)$ on $\mathbf{k}_i$ and ω_i. In the limit of small $\mathbf{k}$, both $\mathbf{k}_1$ and $\mathbf{k}_2$ are restricted to thin caps on the Fermi sphere and, hence, are associated with energies close to the Fermi energy E_0. Since only the energy differences $E_{\mathbf{k}_1}-E_{\mathbf{k}_2}$, $E_{\mathbf{k}_1-\mathbf{k}}-E_{\mathbf{k}_2-\mathbf{k}}$ enter (3.4), we make little error if we replace $\tilde{\epsilon}^L(\mathbf{k}_i,\omega_i)$ by the static dielectric constant $\tilde{\epsilon}^L(\mathbf{k}_i,0)$. The $\mathbf{k}_i$ which enter (3.5) all lie in the interval $0<k_i<2k_0$. Since $\tilde{\epsilon}^L(\mathbf{k}_i,0)$ is real and monotonically decreasing, and behaves as

$$\tilde{\epsilon}^L(\mathbf{k}_i,0)=1+3\omega_p{}^2/k_i{}^2v_0{}^2 \tag{3.6}$$

for small k_i, and as

$$\tilde{\epsilon}^L(2k_0,0)=1+3\omega_p{}^2/2k_i{}^2v_0{}^2 \tag{3.7}$$

for $k_i=2k_0$; it should be a good approximation to use

$$v(\mathbf{k}_i)/\tilde{\epsilon}^L(\mathbf{k}_i,\omega_i)\approx 4\pi e^2/(k_i{}^2+2\alpha k_0{}^2), \tag{3.8}$$

where

$$2\alpha=3\omega_p{}^2/(k_0v_0)^2=4/(\pi k_0a_0). \tag{3.9}$$

Thus, the graphical analysis leads us back to an approximate Yukawa-type screened interaction.[14] The evaluation of (3.5) now proceeds as for (2.6) with the result

[14] A more accurate analysis shows that the potential actually falls off more slowly over large distances than the Yukawa force and behaves as $\cos(2k_0r)/r^3$. See J. Langer and S. Vosko, Phys. Chem. Solids, 12, 196 (1960).

$$\Delta\epsilon_2{}^S=\frac{1}{\pi a_0{}^2k^2}\left\{\left[\frac{2u^2}{[\alpha^2+2\alpha(1-u^2)]^{1/2}}\ln\left|\frac{(1-u)}{(1+u)}\frac{(1+u+\alpha)\{\alpha+[\alpha^2+2\alpha(1-u^2)]^{1/2}\}+\alpha(1-u^2)}{(1-u+\alpha)\{\alpha+[\alpha^2+2\alpha(1-u^2)]^{1/2}\}+\alpha(1-u^2)}\right|\right.\right.$$
$$\left.\left.-2u\alpha\ln\left(\frac{2+\alpha}{\alpha}\right)+4u\right]\eta(1-u)+\left[(1+\alpha)\ln\left(\frac{2+\alpha}{\alpha}\right)-2\right]\delta(1-u)\right\}. \quad (3.10)$$

Figure 4 contains a plot of this expression using $\alpha=\frac{2}{3}$ which is appropriate for an intermediate electron density corresponding to the density of conduction electrons in aluminum. Note that $\Delta\epsilon_2{}^S$ diverges only logarithmically near $u=1$ and the δ function has a finite argument. However, $\Delta\epsilon_2{}^S$ is still not an acceptable correction to the dielectric constant in the region of $u=1$. It is not merely the long-range nature of the Coulomb force which causes perturbation theory to break down, and it is necessary to look at additional high-order processes which might cause difficulty.

In the remainder of this paper we consider graphs for which the same arguments, which led to the effective Yukawa interaction (3.8), seem justified, and thus we continue to use this effective instantaneous force throughout. In this approximation the electron gas can be viewed as a gas of particles which interact via the elementary two-particle Yukawa force (3.8). Then $\Delta\epsilon_2{}^S$ given by (3.10) is the first-order perturbation correction to ϵ_2 for small k, which is completely analogous to (2.8) for a gas with unscreened Coulomb interactions.

For comparison with the unscreened case we give the moments of u calculated with $\Delta\epsilon_2{}^S$. The correction to the zeroth moment again vanishes exactly in accord with the sum rule. The correction to the second moment analogous to (2.16) is

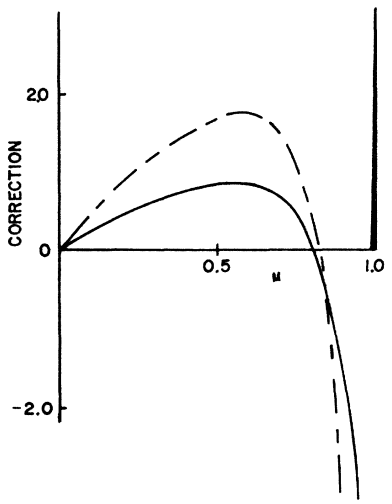

FIG. 4. The screened correction $\Delta\epsilon_2{}^S$ to the imaginary part of Lindhard's dielectric constant in units of $1/(\pi a_0{}^2k^2)$ plotted as a function of u for an electron density equal to the density of conduction electrons in aluminum. This function, which was calculated from the graphs of Fig. 3, is not as singular as the unscreened correction shown by the dashed line, but still violates the positive-definiteness requirement for $u\approx 1$.

$$\Delta^S\langle u^2\rangle=-(1/5\pi k_0a_0)$$
$$\times\{1-2\alpha+(\alpha/2)(1+2\alpha)\ln[(2+\alpha)/\alpha]\}, \quad (3.11)$$

which approaches the unscreened result for small α.

IV. THE EFFECTIVE MASS

Having found an effective interaction between particles we now investigate the effect of using improved single-particle propagators. Note that Figs. 1(c) and (d) are essentially the same as Fig. 1(a), except that in each of these graphs one of the particle propagators contains a self-energy correction. Since the δ function which appears at $u=1$ in $\Delta\epsilon_2$ arises from (2.6b), the contributions of these graphs, one might suspect that higher-order self-energy corrections could individually also give large or singular contributions and hence should be considered.

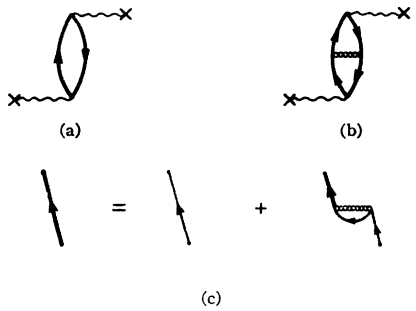

FIG. 5. (a) Zero-order and (b) first-order irreducible skeleton graphs which contribute to the dielectric constant when the effective interaction and effective single-particle propagators are used. The single-particle propagator is taken as the solution of an integral equation represented in (c) and the effective interaction can be approximated by an instantaneous force for small k as indicated in Sec. III.

It is well known[15] that self-energy corrections can be taken into account by replacing the single-particle propagators $S(\mathbf{k}_i,\omega_i)$ by effective propagators $\mathcal{S}(\mathbf{k}_i,\omega_i)$. This procedure is equivalent to another rearrangement of the perturbation series after which only a reduced class of skeleton graphs, without any self-energy parts, are considered, and the new propagators are determined by the sum over all possible graph parts which begin with an incoming particle line $S(\mathbf{k}_i,\omega_i)$, end with an outgoing particle line $S(\mathbf{k}_i,\omega_i)$, and have no other external lines. Alternatively, $\mathcal{S}(\mathbf{k}_i,\omega_i)$ can be found from an integral equation

$$\mathcal{S}(\mathbf{k}_i,\omega_i)=S(\mathbf{k}_i,\omega_i)+S(\mathbf{k}_i,\omega_i)\Sigma(\mathbf{k}_i,\omega_i)\mathcal{S}(\mathbf{k}_i,\omega_i), \quad (4.1)$$

[15] A. Klein and R. Prange, Phys. Rev. 112, 994 (1958).

in terms of the "mass" operator or irreducible self-energy operator $\Sigma(\mathbf{k}_i,\omega_i)$. As noted by Klein[16,17] $\mathcal{S}(\mathbf{k}_i,\omega_i)$ can be expressed in a form which is similar to $S(\mathbf{k}_i,\omega_i)$. Then the rules of Appendix A remain valid except that in rule 2 one must replace $S(\mathbf{k}_i,\omega_i)$ by

$$\mathcal{S}(\mathbf{k}_i,\omega_i)=\frac{i\eta_{\mathbf{k}_i>}}{\omega_i-E_{\mathbf{k}_i}-i\Sigma(\mathbf{k}_i,\omega_i)+i\alpha}+\frac{i\eta_{\mathbf{k}_i<}}{\omega_i-E_{\mathbf{k}_i}-i\Sigma(\mathbf{k}_i,\omega_i)-i\alpha}. \quad (4.2)$$

We take as the effective propagator the solution of the integral equation represented in Fig. 5(c), which contains the first approximation to the mass operator in terms of the effective interaction:

$$\Sigma(\mathbf{k}_i,\omega_i)=\frac{1}{2\pi i\Omega}\sum_{\mathbf{k}_j}\int_{-\infty}^{\infty}d\omega_j \times S(\mathbf{k}_j,\omega_j)\mathcal{U}(\mathbf{k}_i-\mathbf{k}_j,\omega_i-\omega_j). \quad (4.3)$$

We further approximate $\mathcal{U}(\mathbf{k}_i,\omega_i)$ by $\mathcal{U}(\mathbf{k}_i)=v(\mathbf{k}_i)/\tilde{\epsilon}^L(\mathbf{k}_i,\omega_i)$ as given by (3.8), resulting in a $\Sigma(\mathbf{k}_i,\omega_i)$ which is purely imaginary and independent of ω_i. The first two skeleton graphs which arise are shown in Figs. 5(a) and 5(b). Applying the new form of the rules and carrying out the integrations over frequency, we obtain their contributions in the form

$$\epsilon_2{}^{5a}=[2\pi v(\mathbf{k})/\Omega]\sum_{\mathbf{k}_1}\eta_{\mathbf{k}_1>}\eta_{\mathbf{k}_1-\mathbf{k}<}[\delta(\omega-E_{\mathbf{k}_1}{}^*+E_{\mathbf{k}_1-\mathbf{k}}{}^*)-\delta(\omega+E_{\mathbf{k}_1}{}^*-E_{\mathbf{k}_1-\mathbf{k}}{}^*)], \quad (4.4a)$$

$$\epsilon_2{}^{5b}=-\frac{4\pi v(\mathbf{k})}{\Omega^2}\sum_{\mathbf{k}_1,\mathbf{k}_2}\eta_{\mathbf{k}_1>}\eta_{\mathbf{k}_1-\mathbf{k}<}\eta_{\mathbf{k}_2>}[\delta(\omega-E_{\mathbf{k}_1}{}^*+E_{\mathbf{k}_1-\mathbf{k}}{}^*)-\delta(\omega+E_{\mathbf{k}_1}{}^*-E_{\mathbf{k}_1-\mathbf{k}}{}^*)] \times\left(\frac{\mathcal{U}(\mathbf{k}_1-\mathbf{k}_2-\mathbf{k})\eta_{\mathbf{k}_2+\mathbf{k}<}}{E_{\mathbf{k}_2+\mathbf{k}}{}^*-E_{\mathbf{k}_2}{}^*-E_{\mathbf{k}_1}{}^*+E_{\mathbf{k}_1-\mathbf{k}}{}^*}-\mathcal{P}\frac{\mathcal{U}(\mathbf{k}_1-\mathbf{k}_2)\eta_{\mathbf{k}_2-\mathbf{k}<}}{E_{\mathbf{k}_2}{}^*-E_{\mathbf{k}_2-\mathbf{k}}{}^*-E_{\mathbf{k}_1}{}^*+E_{\mathbf{k}_1-\mathbf{k}}{}^*}\right), \quad (4.4b)$$

where

$$E_{\mathbf{k}}{}^*=k^2/(2m)+i\Sigma(\mathbf{k}), \quad (4.5)$$

and the redundant frequency dependence of $\Sigma(\mathbf{k},\omega)$ has been suppressed. Except for the appearance of $E_{\mathbf{k}}{}^*$'s in place of $E_{\mathbf{k}}$'s these terms are identical to expressions we have previously encountered. The first gave rise to Lindhard's $\epsilon_2{}^L(\mathbf{k},\omega)$, and (4.4b) resembles (2.6a). The term (2.6b) has no counterpart in the present scheme since its contribution has been absorbed into (4.4a).

Note that only energy differences of the form $E_{\mathbf{k}_1}{}^*-E_{\mathbf{k}_1-\mathbf{k}}{}^*$ enter into Eqs. (4.4), and in each case $\mathbf{k}_1$ (also $\mathbf{k}_2$) is restricted to values outside the Fermi sea and $\mathbf{k}_1-\mathbf{k}$ to values within the sea. As a result, in the small-$\mathbf{k}$ limit $\mathbf{k}_1$ takes on values within a very thin cap on the Fermi sea. The relevant energy differences are easily evaluated for this case. Introducing an effective mass m^* and explicitly evaluating $i[\Sigma(\mathbf{k}_1)-\Sigma(\mathbf{k}_1-\mathbf{k})]$, we find to first order in k

$$E_{\mathbf{k}_1}{}^*-E_{\mathbf{k}_1-\mathbf{k}}{}^*=\mathbf{k}_1\cdot\mathbf{k}/m^*, \quad (4.6)$$

where

$$1/m^*=(1/m)\{1-(1/2\pi k_0a_0)\times[2-(1+\alpha)\ln(2+\alpha)/\alpha]\}, \quad (4.7)$$

or, using (3.9),

$$m^*/m=\{1-(\alpha/4)[2-(1+\alpha)\ln(2+\alpha)/\alpha]\}^{-1}. \quad (4.8)$$

m^*/m is plotted in Fig. 6 as a function of α. For these graphs the effective mass is equal to the electron mass for $\alpha=0$ and for very large α, while for intermediate coupling it is smaller, but never departs from m by more than 5%.

The Lindhard self-energy corrected ϵ_2 now becomes [compare (2.3)]

$$\epsilon_2{}^{5a}=(2k_0/a_0k^2)(m^*/m)u'\eta(1-|u'|), \quad (4.9)$$

where

$$u'=u(m^*/m)=m^*\omega/(kk_0). \quad (4.10)$$

However, this function by itself no longer satisfies the sum rule (2.12), but must be augmented by $\epsilon_2{}^{5b}$,

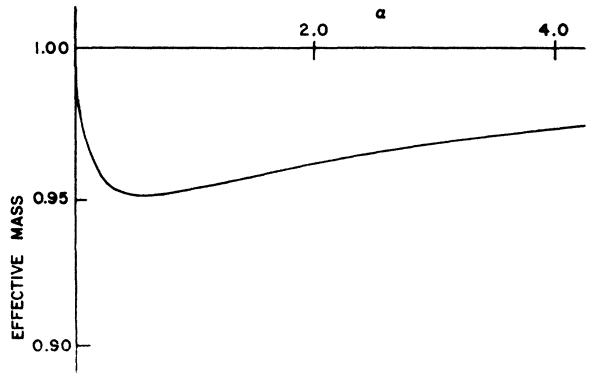

FIG. 6. The ratio of the effective mass to the electron mass as a function of the dimensionless screening constant α. The effective mass is smaller than m, but doesn't depart from it by more than 5%. For $\alpha=0$ and very large α the effective mass equals the electron mass. The numerical calculations of the dielectric constant reported later in this paper are for $\alpha=\frac{2}{3}$. In this region the difference between m and m^* is most pronounced.

[16] A. Klein, in *Lectures on the Many Body Problem, Naples, 1960*, edited by E. R. Caianiello (Academic Press Inc., New York, to be published).

[17] Note that the present definitions of $S(\mathbf{k},\omega)$ and $\Sigma(\mathbf{k},\omega)$ are consistent with references 4, 5, and 7, but differ by a factor of i from those used in references 15 and 16.

$$\epsilon_2{}^{5b}=\frac{2}{\pi a_0{}^2k^2}\left(\frac{m^*}{m}\right)^2\eta(1-|u'|)\left\{u'\ln\left(\frac{2+\alpha}{\alpha}\right)\right.$$
$$\left.+\frac{u'^2}{[\alpha^2+2\alpha(1-u'^2)]^{1/2}}\ln\left(\frac{(1-u')}{(1+u')}\frac{(1-u'+\alpha)\{\alpha+[\alpha^2+2\alpha(1-u'^2)]^{1/2}\}+\alpha(1-u'^2)}{(1+u'+\alpha)\{\alpha+[\alpha^2+2\alpha(1-u'^2)]^{1/2}\}+\alpha(1-u'^2)}\right)\right\}. \quad (4.11)$$

Combining (4.9) and (4.11) and using (3.9) we find the imaginary part of the self-energy corrected dielectric constant $\epsilon_2{}^{SE}$:

$$\epsilon_2{}^{SE}=\frac{2k_0}{a_0k^2}\left(\frac{m^*}{m}\right)\eta(1-|u'|)u'\left\{1+\frac{\alpha}{2}\left(\frac{m^*}{m}\right)\left[\ln\left(\frac{2+\alpha}{\alpha}\right)\right.\right.$$
$$\left.\left.+\frac{u'}{[\alpha^2+2\alpha(1-u'^2)]^{1/2}}\ln\left(\frac{(1-u')}{(1+u')}\frac{(1-u'+\alpha)\{\alpha+[\alpha^2+2\alpha(1-u'^2)]^{1/2}\}+\alpha(1-u'^2)}{(1+u'+\alpha)\{\alpha+[\alpha^2+2\alpha(1-u'^2)]^{1/2}\}+\alpha(1-u'^2)}\right)\right]\right\}. \quad (4.12)$$

$\epsilon_2{}^{SE}$ is plotted in Fig. 7 with $\alpha=\frac{2}{3}$. Note, in comparison with Figs. 2 and 4, that the δ function at $u=1$ no longer appears, but that the largest contributing frequency has been shifted from $u=1$ to $u\approx1.05$. This shift reflects a small change in the single-particle energy of particles near the Fermi surface due to interaction between the electrons. The singularities which arise in the pure perturbative approach, with Figs. 1(c) and (d) contributing δ-function peaks to ϵ_2 and higher order terms giving rise to derivatives of δ functions, provide a rather violent indication that these energy shifts occur, but their accurate treatment can only be accomplished by means of a formal mass renormalization as carried out above.

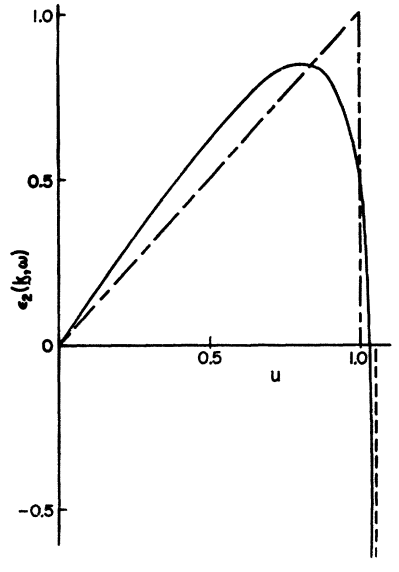

FIG. 7. Imaginary part of the dielectric constant calculated from the graphs of Fig. 5. Here $\epsilon_2{}^{SE}(\mathbf{k},\omega)$ is plotted in units of $2k_0/(a_0k^2)$ and as a function of u for an electron density equal to the density of conduction electrons in aluminum. There is no δ-function peak in this approximation and the highest u for which ϵ_2 is not zero has been shifted from $u=1$ to $u\approx1.05$. However, this approximation continues to exhibit the logarithmic singularity which causes a violation of the positive-definiteness requirement. The broken line shows the zero-order ϵ_2.

Though $\epsilon_2{}^{SE}$ provides an improved approximation to the imaginary part of the dielectric constant it still contains a logarithmic divergence which tends to drive it negative for u near its maximum value. Thus, a further refinement of the calculation is necessary to obtain a positive-definite ϵ_2. We proceed with this calculation in the next section after recording two moments of $\epsilon_2{}^{SE}$:

$$\langle u^0\rangle_{k\to0}{}^{SE}=1, \quad (4.13)$$

$$\langle u^2\rangle_{k\to0}{}^{SE}=\frac{3}{5}\left(\frac{m}{m^*}\right)^3\left\{1+\frac{2}{\pi k_0a_0}\frac{m}{m^*}\right.$$
$$\left.\times\left[\frac{4+\alpha}{3}-\tfrac{1}{12}(2\alpha^2+10\alpha+9)\ln\left(\frac{2+\alpha}{\alpha}\right)\right]\right\}. \quad (4.14)$$

Equation (4.13) is in agreement with the sum rule (2.12) and it holds independent of whether α is chosen to have the specific value (3.9) or is just retained as an arbitrary screening parameter. Using (3.9) and (4.8), the second moment reduces to the DuBois result (2.14) in the high-density limit ($\alpha\to0$):

$$\langle u^2\rangle_{k\to0}{}^{SE}\underset{\alpha\to0}{\longrightarrow}\tfrac{3}{5}(1-\alpha/6). \quad (4.15)$$

V. THE CORRECTION TO ϵ_2

The contributions of Figs. 5(a) and (b) to the matrix element needed for ϵ_2 can be expressed in the form

$$\text{M.E.}^5=-\frac{i}{\pi}\int_{-\infty}^{\infty}d\omega'\,e^{-i\omega' t}$$
$$\times\sum_{\mathbf{k}_1}[F(\mathbf{k}_1,\mathbf{k},\omega')+(1/\Omega)F(\mathbf{k}_1,\mathbf{k},\omega')$$
$$\times\sum_{\mathbf{k}_2}v(\mathbf{k}_1-\mathbf{k}_2)F(\mathbf{k}_2,\mathbf{k},\omega')], \quad (5.1)$$

where $F(\mathbf{k}_1,\mathbf{k},\omega')$ is related to the propagator for a mass corrected, but otherwise free, particle and hole:

$$F(\mathbf{k}_1,\mathbf{k},\omega')$$
$$=\frac{1}{2\pi i}\int_{-\infty}^{\infty}d\omega_1\, \mathcal{S}(\mathbf{k}_1-\mathbf{k},\omega_1-\omega')\mathcal{S}(\mathbf{k}_1,\omega_1)$$
$$=\frac{\eta_{\mathbf{k}_1-\mathbf{k}}>\eta_{\mathbf{k}_1}<}{\omega'-E_{\mathbf{k}_1}{}^*+E_{\mathbf{k}_1-\mathbf{k}}{}^*-i\lambda}-\frac{\eta_{\mathbf{k}_1-\mathbf{k}}<\eta_{\mathbf{k}_1}>}{\omega'-E_{\mathbf{k}_1}{}^*+E_{\mathbf{k}_1-\mathbf{k}}{}^*+i\lambda}$$
$$=\frac{\eta_{\mathbf{k}_1-\mathbf{k}}>\eta_{\mathbf{k}_1}<}{\omega'-\mathbf{k}\cdot\mathbf{k}_1/m^*-i\lambda}-\frac{\eta_{\mathbf{k}_1-\mathbf{k}}<\eta_{\mathbf{k}_1}>}{\omega'-\mathbf{k}\cdot\mathbf{k}_1/m^*+i\lambda}. \quad (5.2)$$

For small $\mathbf{k}$ this propagator has a pole for $\omega'\approx kk_0/m^*$ which can be associated with the tendency of particles and holes to form bound states. It is the presence of this pole which causes the second term on the right of Eq. (5.1) to become large, signaling the breakdown of perturbation theory for $u'\approx 1$. In order to properly account for the bound state it is necessary to use a better propagator which incorporates repeated particle-hole scatterings. Thus, we now include the set of graphs shown in Fig. 8. Applying the rules of Appendix A and using the effective interaction of Sec. III and the propagators of Sec. IV, we can express the contribution of these graphs in a form analogous to (5.1):

$$\text{M.E.}^8=-\frac{i}{\pi}\int_{-\infty}^{\infty}d\omega'\, e^{-i\omega' t}\sum_{\mathbf{k}_1}G(\mathbf{k}_1,\mathbf{k},\omega'), \quad (5.3)$$

where

$$G(\mathbf{k}_1,\mathbf{k},\omega')$$
$$=F(\mathbf{k}_1,\mathbf{k},\omega')+\frac{1}{\Omega}F(\mathbf{k}_1,\mathbf{k},\omega')\sum_{\mathbf{k}_2}\mathcal{U}(\mathbf{k}_1-\mathbf{k}_2)F(\mathbf{k}_2,\mathbf{k},\omega')$$
$$+\frac{1}{\Omega^2}F(\mathbf{k}_1,\mathbf{k},\omega')\sum_{\mathbf{k}_2}\mathcal{U}(\mathbf{k}_1-\mathbf{k}_2)F(\mathbf{k}_2,\mathbf{k},\omega')$$
$$\times\sum_{\mathbf{k}_3}\mathcal{U}(\mathbf{k}_2-\mathbf{k}_3)F(\mathbf{k}_3,\mathbf{k},\omega')+\frac{1}{\Omega^3}F(\mathbf{k}_1,\mathbf{k},\omega')$$
$$\times\sum_{\mathbf{k}_2}\mathcal{U}(\mathbf{k}_1-\mathbf{k}_2)F(\mathbf{k}_2,\mathbf{k},\omega')\sum_{\mathbf{k}_3}\mathcal{U}(\mathbf{k}_2-\mathbf{k}_3)$$
$$\times F(\mathbf{k}_3,\mathbf{k},\omega')\sum_{\mathbf{k}_4}\mathcal{U}(\mathbf{k}_3-\mathbf{k}_4)F(\mathbf{k}_4,\mathbf{k},\omega')+\cdots. \quad (5.4)$$

$G(\mathbf{k}_1,\mathbf{k},\omega')$ is related to the propagator for an interacting particle and hole, and Eq. (5.4) is equivalent to the integral equation

$$G(\mathbf{k}_1,\mathbf{k},\omega')$$
$$=F(\mathbf{k}_1,\mathbf{k},\omega')+\frac{1}{\Omega}F(\mathbf{k}_1,\mathbf{k},\omega')$$
$$\times\sum_{\mathbf{k}_2}\mathcal{U}(\mathbf{k}_1-\mathbf{k}_2)G(\mathbf{k}_2,\mathbf{k},\omega'). \quad (5.5)$$

Removing a factor of $F(\mathbf{k}_1,\mathbf{k},\omega')$ from $G(\mathbf{k}_1,\mathbf{k},\omega')$, we write

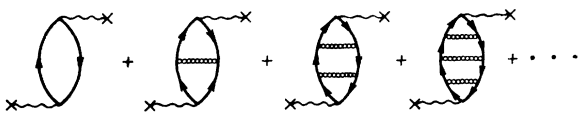

FIG. 8. Graphs which give rise to a positive-definite corrected ϵ_2. These graphs account for repeated scatterings of effective particles and holes via the effective-interparticle interaction.

$$G(\mathbf{k}_1,\mathbf{k},\omega')=F(\mathbf{k}_1,\mathbf{k},\omega')H(\mathbf{k}_1,\mathbf{k},\omega'). \quad (5.6)$$

Then $H(\mathbf{k}_1,\mathbf{k},\omega')$ satisfies

$$H(\mathbf{k}_1,\mathbf{k},\omega')=1+(1/\Omega)\sum_{\mathbf{k}_2}\mathcal{U}(\mathbf{k}_1-\mathbf{k}_2)$$
$$\times F(\mathbf{k}_2,\mathbf{k},\omega')H(\mathbf{k}_2,\mathbf{k},\omega'). \quad (5.7)$$

In the neighborhood of $\omega'=kk_0/m^*$ one might expect that $F(\mathbf{k}_1,\mathbf{k},\omega')$ dominates the behavior of $G(\mathbf{k}_1,\mathbf{k},\omega')$ and $H(\mathbf{k}_1,\mathbf{k},\omega')$ is essentially constant and can be taken out of the sum in (5.7). Thus, in this region,

$$H(\mathbf{k}_1,\mathbf{k},\omega')\approx 1+(1/\Omega)H(\mathbf{k}_1,\mathbf{k},\omega')$$
$$\times\sum_{\mathbf{k}_2}\mathcal{U}(\mathbf{k}_1-\mathbf{k}_2)F(\mathbf{k}_2,\mathbf{k},\omega'). \quad (5.8)$$

This latter equation is readily solved and gives

$$G(\mathbf{k}_1,\mathbf{k},\omega')\approx\frac{F(\mathbf{k}_1,\mathbf{k},\omega')}{1-(1/\Omega)\sum_{\mathbf{k}_2}\mathcal{U}(\mathbf{k}_1-\mathbf{k}_2)F(\mathbf{k}_2,\mathbf{k},\omega')}. \quad (5.9)$$

Away from the singular region the perturbation series seems to be adequate to determine the corrected form of ϵ_2. We now show that in this case too Eq. (5.9) provides an accurate solution for $G(\mathbf{k}_1,\mathbf{k},\omega')$.

When expanded, (5.9) reproduces the first two terms on the right-hand side of (5.4). By interchanging the dummy indices $\mathbf{k}_1\leftrightarrow\mathbf{k}_2$ it can be seen that the third term on the right is also given correctly when summed over $\mathbf{k}_1$ as in (5.3). Thus, the approximation only begins with the fourth term corresponding to the last bubble shown in Fig. 8 and should be very good for the whole range of frequency. In the particular case when the screening becomes very strong ($\alpha\gg 1$) so that $\mathcal{U}(\mathbf{k})$ becomes essentially a constant independent of $\mathbf{k}$, then (5.9) becomes an exact solution for $G(\mathbf{k}_1,\mathbf{k},\omega')$.

Utilizing the techniques of Appendix B to bypass the ω' and t integrations, we obtain

$$\epsilon_2(\mathbf{k},\omega)=\frac{2k_0}{\pi a_0k^2}\left(\frac{m^*}{m}\right)\text{Im}\int_{-1}^{1}dx$$
$$\times\frac{x}{x-u'-i\lambda}\frac{1}{1+I(u',x)}, \quad (5.10)$$

where λ is an infinitesimal. The frequency dependence in (5.10) is represented by u' which was defined in (4.10), and the real and imaginary parts, I_1 and I_2 of $I(u',x)$ are given by

$$I_1=\frac{m^*/m}{2\pi k_0 a_0}\left\{\ln\left(\frac{\alpha}{2+\alpha}\right)+\frac{u'}{[(u'-x)^2+2\alpha(1-xu')+\alpha^2]^{1/2}}\right.$$
$$\left.\times\ln\left(\frac{(1+u')}{(1-u')}\frac{(u'-x)(1-x)+\alpha(2-xu'-x)+\alpha^2+(1-x+\alpha)[(u'-x)^2+2\alpha(1-xu')+\alpha^2]^{1/2}}{(u'-x)(1+x)-\alpha(2-xu'+x)-\alpha^2-(1+x+\alpha)[(u'-x)^2+2\alpha(1-xu')+\alpha^2]^{1/2}}\right)\right\} \quad (5.11a)$$

$$I_2=-\frac{m^*/m}{2k_0a_0}\eta(1-|u'|)\frac{u'}{[(u'-x)^2+2\alpha(1-xu')+\alpha^2]^{1/2}}. \quad (5.11b)$$

Equation (5.10) has been numerically evaluated for an electron density equal to the density of conduction electrons in aluminum and the result is plotted in Fig. 9. Note that there is a sizable departure from the Lindhard $\epsilon_2{}^L$ for this electron density, as might be expected, but the violent fluctuations characterizing the previous incomplete approximations have disappeared. ϵ_2 is positive definite and the values obtained for the moments are shown in the table where they are compared with the corresponding moments for different approximations. Note that the zeroth moment, which represents the sum rule (2.12), is satisfied to within $2\frac{1}{2}\%$ and provides an indication of the numerical accuracy of the dielectric constant we have obtained and of the other moments.

The corresponding real part of the dielectric constant has been computed from the Kramers-Kronig relation, Eq. (2.2) and is plotted and compared with the Lindhard $\epsilon_1{}^L$ in Fig. 10. For small u the corrected dielectric constant departs appreciably from $\epsilon_1{}^L$. The zero-frequency value is fixed by the moment $\langle u^{-2}\rangle$:

$$\epsilon_1(\mathbf{k},0)-1=u_p{}^2\langle u^{-2}\rangle, \quad (5.12)$$

and is thus shifted by 20%. For frequencies near kv_0 there is a rapid variation in ϵ_1, but it no longer becomes negative infinite. At higher frequencies the changes in the dielectric constant due to the correction are small but, nevertheless, can be important in certain cases, as for determining properties of the plasmon excitation mode. Since ϵ_2 vanishes for high frequencies in this approximation, we can obtain the asymptotic behavior of ϵ_1 in terms of the even moments of ϵ_2:

$$\epsilon_1(\mathbf{k},\omega)\underset{u\to\infty}{\longrightarrow}1-(u_p{}^2/u^2)\times\{1+\langle u^2\rangle/u^2+\langle u^4\rangle/u^4+\cdots\}. \quad (5.13)$$

It has been observed that a rather good empirical fit (within 5%) to the dielectric constant shown in Fig. 9 is given by

$$\epsilon_2{}^{\text{fit}}=(2k_0/k^2a_0)\tfrac{3}{2}u'(1-u'^2)^{1/2},\quad 0<u'<1. \quad (5.13)$$

This function can be used for rough calculations of properties of the electron gas for an aluminum electron density, though the analytical behavior near $u'=1$ is probably not correctly represented by (5.13). The Kramers-Kronig relation gives for the corresponding real part

$$\epsilon_1{}^{\text{fit}}=(2k_0/k^2a_0)\tfrac{3}{2}(\tfrac{1}{2}-u'^2),\quad u'^2<1$$
$$=(2k_0/k^2a_0)\tfrac{3}{2}[\tfrac{1}{2}-u'^2+u'(u'^2-1)^{1/2}],\quad u'^2>1. \quad (5.14)$$

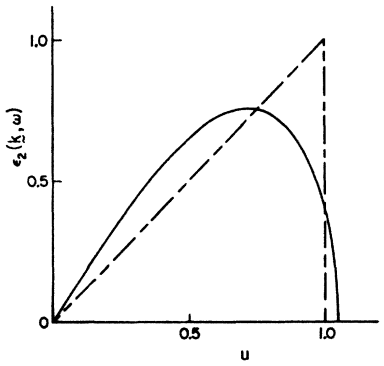

FIG. 9. Imaginary part of the corrected dielectric constant calculated from the graphs of Fig. 8, and plotted in units of $2k_0/(a_0k^2)$ as a function of u for an electron density equal to the density of conduction electrons in aluminum. For this electron density ϵ_2 departs appreciably from the Lindhard form shown by the broken line, but is well behaved and no longer exhibits the violent fluctuations characterizing the previous incomplete approximations.

VI. SUMMARY

We have derived the dielectric constant of the interacting degenerate electron gas moving in a uniform positive background of charge. In order to obtain an acceptable function which does not violate the sum rule and positive-definiteness restrictions on the imaginary part it was necessary to include three types of corrections to previous calculations. These corrections (1) account for the effect of higher order processes which tend to screen the long-range elementary Coulomb interactions; (2) provide for the shift in single-particle energies which manifests itself as a change in the effective mass of particles and holes; and (3) allow for the presence of a particle-hole bound state by treating the repeated or "t-matrix" scattering of particles and holes.

Numerical calculations of the dielectric constant and moments of ϵ_2 were carried out for an intermediate electron density equivalent to the density of conduction electrons in aluminum. The resulting dielectric constant departs considerably from the Lindhard form for low frequencies, but has similar qualitative features. The moments can be used to determine the high-

frequency behavior and other properties of the electron gas. However, the small wave number limit was used to simplify the numerical calculations. The extension to finite wave numbers presents a substantial computational problem, but would be necessary to find the effect of the corrections on properties such as the correlation energy and the pair-distribution function. A preliminary step in this direction is being carried out by Hubbard and Leigh[18] who are calculating the wave-number dependence of the static dielectric constant.[18a]

There is some question of the validity of applying the present approximations to metallic electron densities since they are based on a partially summed perturbation series and there is no guarantee that neglected higher order terms are not significant. However, the fact that even the Lindhard approximation provides such a qualitatively and often quantitatively accurate description of many properties of real metals would indicate that any correction terms should be well behaved and that they should not alter the general structure of the dielectric constant appreciably. The present corrected form indeed satisfies this criterion and appears to lead to results in better accord with the experimental information available. Recently, Baym and Kadanoff[19] have emphasized the importance of preserving certain conservation laws in the approximations used for many-body calculations. The present calculation is essentially in accord with their criteria and contains the same type of terms as contribute to their two-particle correlation function when calculated in what they call the generalized random-phase approximation. However, for the electron gas it appears necessary to include, in addition, a screening of the long-range Coulomb interaction between particles in order to obtain well-behaved results.

ACKNOWLEDGMENTS

Much of the work reported in this paper was carried out while the author was a National Science Foundation Postdoctoral Fellow at the Weizmann Institute of Science. I would like to acknowledge the hospitality of that Institution and numerous discussions with its scientists and fellows, in particular with my office companion A. Reiner. I also enjoyed the hospitality of the Institute of Theoretical Physics of the University of Copenhagen and the A. E. R. E. at Harwell during the Summer of 1961, and at the latter Institution benefited particularly from discussions with J. Hubbard and R. Leigh. Finally, I would like to thank D. Falk, R. Ferrell, and R. Prange for many stimulating discussions, and D. Falk for a critical reading of the manuscript.

[18] J. Hubbard and R. Leigh (private communication).

[18a] *Note added in proof.* It has been brought to the author's attention that the same higher order diagrams as considered in this paper have been studied by Y. Osaka, J. Phys. Soc. Japan **17**, 546 and 1322(E) (1962). Osaka's calculations, however, are restricted to both the small wave number and small frequency limits.

[19] G. Baym and L. P. Kadanoff, Phys. Rev. **124**, 287 (1962).

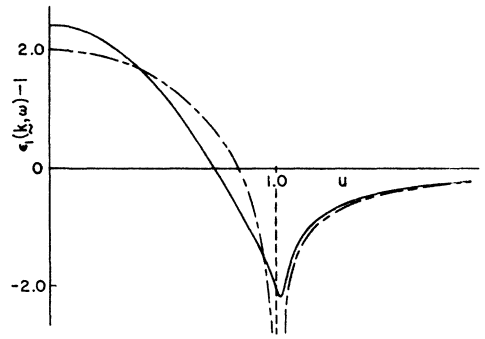

FIG. 10. Real part of the dielectric constant minus 1 in units of $2k_0/(\pi a_0 k^2)$ as found from the corrected ϵ_2 of Fig. 9 by means of the Kramer-Kronig dispersion relation. For u greater than one this function is very similar to the Lindhard approximation which is shown by the broken line.

APPENDIX A

This Appendix contains rules for finding the contributions of individual graphs to the matrix element of Eq. (2.1). The graphs are drawn as in references 4 and 5, but it is now more convenient to label the directed particle lines and the dashed interaction lines by the momentum $\mathbf{k}_i$ and frequency ω_i they carry. Choose an arbitrary direction for the flow of momentum and energy along the interaction lines, and label the $\rho_{\mathbf{k}}$ lines by $\mathbf{k}$ and ω' such that the lower ρ line is directed into its vertex and the upper ρ line out of its vertex. The labeling should be such as to conserve momentum and frequency at each vertex. Then the contribution of the graph is given by:

(1) a factor $v(\mathbf{k}_i)/(2\pi i\Omega)$ for an interaction line marked $(\mathbf{k}_i,\omega_i)$;

(2) a factor

$$S(\mathbf{k}_i,\omega_i)=\frac{i\eta_{\mathbf{k}_i>}}{\omega_i-E_{\mathbf{k}_i}+i\lambda}+\frac{i\eta_{\mathbf{k}_i<}}{\omega_i-E_{\mathbf{k}_i}-i\lambda} \tag{A1}$$

for a directed line marked $(\mathbf{k}_i,\omega_i)$, where

$$\begin{aligned}\eta_{\mathbf{k}_i<}&=1 \quad \text{for} \quad |\mathbf{k}_i|<k_0\\ &=0 \quad \text{otherwise},\\ \eta_{\mathbf{k}_i>}&=1 \quad \text{for} \quad |\mathbf{k}_i|>k_0\\ &=0 \quad \text{otherwise},\end{aligned}$$

and $E_{\mathbf{k}_i}=k_i^2/2m$;

(3) a factor $\exp(-i\omega' t/2)/2\pi$ for each ρ line;

(4) summation over all $\mathbf{k}_i$ but not $\mathbf{k}$, and integration of all ω_i and ω' over the interval $(-\infty, \infty)$;

(5) multiplication by a factor $(-2)^l$, where l is the number of closed particle loops. The 2 accounts completely for the two spin states of the electrons, and no other sum over spins should be carried out.

The contribution to the matrix element obtained by application of the above rules contains integrals over frequencies ω_i and ω', and sums over momenta $\mathbf{k}_i$. An

additional integration over t is required to find the corresponding contribution to ϵ_2. These integrals are not all well defined and it is advisable to use the following prescribed order of integration to obtain the correct result: Integrate, respectively, over the ω_i, t, ω', and finally sum over the $\mathbf{k}_i$. In many cases the integrals over t and ω' can be obviated, as shown in Appendix B. After all of the frequency integrations have been performed the small quantities λ in the particle propagators can be set equal to zero.

APPENDIX B

In this Appendix we note how the integrations over t and ω' in the calculation of ϵ_2 can often be carried out very simply. Neglecting the $\mathbf{k}$ dependence and after carrying out the ω_i integrations one obtains an expression of the form

$$I(\omega)=\mathrm{Re}(i)\int_0^\infty dt\,(e^{i\omega t}-e^{-i\omega t})\int_{-\infty}^\infty d\omega'\,e^{-i\omega' t}F(\omega',\lambda). \quad \text{(B1)}$$

Since $F(\omega',\lambda)$ is the result of integrations over products of $S(\mathbf{k}_i,\omega_i)$ as given by (A1) it can be broken up by means of partial fractions into two parts,

$$F(\omega',\lambda)=F_+(\omega'+i\lambda)+F_-(\omega'-i\lambda),$$

where $F_+(\omega'+i\lambda)$ has denominators containing ω' and the positive infinitesimal λ's in the combination $\omega'+i\lambda$ and hence is analytic in the upper half of the complex ω' plane and $F_-(\omega'-i\lambda)$ is analytic to the lower half of the ω' plane, and each part vanishes for large ω' at least as fast as $|\omega'|^{-1}$. For all the corrections considered in this paper each individual graph or pair of graphs (for the self-energy terms) has the property that $F(\omega',\lambda)$ is even in ω'. In this case, and if $F_\pm(\omega'\pm i\lambda)$ contains no multiple poles, the result of the integrations in (B1) takes a particularly simple form. Integrating over t and then ω' we obtain

$$I(\omega)=-2\pi\,\mathrm{Im}[F_+(\omega+i\lambda)-F_-(\omega-i\lambda)]. \quad \text{(B2)}$$

Since only the imaginary part of the bracket is needed we can use the identities

TABLE I. Moments of ϵ_2. Several moments $\langle u^n\rangle$ calculated in the small-wave-number limit and for $\alpha=2/3$ are compared in the Lindhard, DuBois, and present approximations.

n	Lindhard	DuBois	Present
−2	3.00	4.00	3.57
−1	1.50	1.59	1.60
0	1.00	1.00	0.976
1	0.750	0.693	0.689
2	0.600	0.533	0.529
3	0.500	0.443	0.428
4	0.429	0.391	0.359

$$\mathrm{Im}[-F_-(\omega-i\lambda)]=\mathrm{Im}[F_-(\omega-i\lambda)^*]=\mathrm{Im}[F_-(\omega+i\lambda)],$$

so that

$$I(\omega)=-2\pi\,\mathrm{Im}[F_+(\omega+i\lambda)+F_-(\omega+i\lambda)], \quad \text{(B3)}$$

i.e., the effect of the t and ω' integrals is to change the sign of $i\lambda$ throughout F_- and multiply by 2π.

If $F(\omega,\lambda)$ contains multiple poles as for the self-energy graphs Figs. 1(c) and (d) it is not possible to use the above simple scheme. However, after integrating over t, the ω' integration can still be unambiguously carried out by breaking $F(\omega',\lambda)$ into $F_\pm(\omega'\pm i\lambda)$ and expressing each part as a multiple derivative of a product of simple poles. As an example, consider the following integration:

$$\mathrm{Re}\int_{-\infty}^\infty d\omega'\,\frac{1}{\omega'-\omega-i\lambda}\,\frac{1}{(\omega'-\Delta_1+i\lambda)^{n+1}}\,\frac{1}{(\omega'-\Delta_2+i\lambda)^{m+1}}$$

$$=\frac{d^n}{d\Delta_1{}^n}\frac{d^m}{d\Delta_2{}^m}\mathrm{Re}\int_{-\infty}^\infty d\omega'\,\frac{1}{\omega'-\omega-i\lambda}\,\frac{1}{\omega'-\Delta_1+i\lambda}\,\frac{1}{\omega'-\Delta_2+i\lambda}$$

$$=\frac{d^n}{d\Delta_1{}^n}\frac{d^m}{d\Delta_2{}^m}\mathrm{Re}\left[2\pi i\,\frac{1}{\omega-\Delta_1+i\lambda'}\,\frac{1}{\omega-\Delta_2+i\lambda'}\right]$$

$$=2\pi\left[\mathcal{P}(-1)^m\frac{\delta^m(\omega-\Delta_2)}{(\omega-\Delta_1)^n}-\mathcal{P}(-1)^n\frac{\delta^n(\omega-\Delta_1)}{(\omega-\Delta_2)^m}\right],$$

where

$$\delta^m(\omega-\Delta_2)\equiv(d^m/d\omega^m)\delta(\omega-\Delta_2).$$